Improving Line Crew Dispatch Accuracy When Using Traveling-Wave Fault Locators

Bogdan Kasztenny
Schweitzer Engineering Laboratories, Inc.

Presented at the
46th Annual Western Protective Relay Conference
Spokane, Washington
October 22–24, 2019

Originally presented at the
22nd Annual Georgia Tech Fault and Disturbance Analysis Conference, April 2019

Improving Line Crew Dispatch Accuracy When Using Traveling-Wave Fault Locators

Bogdan Kasztenny
Schweitzer Engineering Laboratories, Inc.

***Abstract*—Traveling-wave (TW) fault locators continue to gain popularity as new economical fault-locating solutions enter the market. These fault locators have a field-proven potential for accuracy on the order of one tower span. When dispatching line crews to inspect and repair the line after a fault, utilities need a simple and accurate method of converting the per-unit fault location from the TW fault locator into a tower position in the physical world if they want to retain the inherent per-unit fault-locating accuracy.**

This paper presents several practical methods for improving the dispatch accuracy. One method uses line faults for which line crews confirmed the fault location with confidence. The method maps a tower with a confirmed fault to the per-unit location of the fault. Such a tower becomes a landmark to help map other towers with improved accuracy. Another method uses a commissioning or troubleshooting report for the fiber-optic cable in the ground wire of the line. As a part of commissioning or troubleshooting fiber cables, utilities measure losses using Optical Time-Domain Reflectometry (OTDR). The OTDR measurements allow locating towers with splices. In our method, these towers become landmarks to map other towers with accuracy.

I. Introduction

Fault locators for power lines have been available for many decades. They have improved considerably in terms of affordability, ease of use, and accuracy [1]. Most recently, traveling-wave (TW) fault locators have been deployed in large numbers.

Any fault locator based on electrical measurements from one or both ends of the line intrinsically operates on a per-unit scale. Historically, such per-unit output has been multiplied by the end-to-end line length to provide a *distance to the fault*, or a *fault location*.

However, as we will discuss and illustrate in this paper, the end-to-end line length is not easy to measure and is typically not known with high accuracy. This becomes bluntly obvious when considering lines spanning between two utilities. Quite often two utilities will know the length of the same line with a difference of 1 to 2 km or mi.

When using impedance-based fault locators, accuracy of the line length is not a primary concern. These fault locators exhibit much larger method errors (impact of fault resistance and its variability, for example) and errors in the line impedances, especially the zero-sequence impedance, than errors in the line length. As a result, our industry did not need to refine its line length estimating methods for obtaining very accurate line length data.

TW fault locators are very accurate, and the issue of line length accuracy is much more significant when applying these fault locators. By eliminating the other more significant errors, the TW fault locators benefit from accurate line length data significantly more than the other fault locators.

However, the quest for more precise end-to-end line length should not be our only objective. What we truly need is accurate location of each tower along the line so that we can associate (map) the output from the TW fault locator to the tower identifier, and from there, to the tower location in the physical world, such as by using Global Positioning System (GPS) coordinates. The need for such mapping of the fault locator output to tower identifiers can be better understood by considering locating faults on highly nonhomogeneous lines. TW fault locators are so accurate that the natural variations in the tower span become a form of nonhomogeneity. You can consider the mapping of per-unit fault location to the tower identifier as *calibration* of the complete fault-locating system. With this understanding, the system comprises the fault locator and adequate detail about the line data.

In this paper, we provide several methods for this calibration process, including the initial calibration as well as ongoing refinements based on line faults.

Section II reviews the operating principles of the single-ended and double-ended TW fault locators, explains their inherently high accuracy in terms of the per-unit output, and reviews and prioritizes sources of fault-locating errors.

Section III reviews several definitions of line length and distance to any given tower, including electrical and geometrical distances, and discusses how we can obtain these distances with accuracy. The section explains a line energization test for obtaining the TW line propagation time – one of the most unambiguous and accurate electrical measures of the end-to-end line length.

Section IV discusses line-end considerations. Where does a power line begin and end in the context of fault locating? At the terminals of the fault locator? At the secondary terminals of the current transformer (CT)? At the first tower? These points may be spaced by a distance that is comparable with the accuracy of the TW fault locator, and therefore these distances should no longer be neglected. The section shows how to account for the line ends, and it advocates for using CT locations as line ends to simplify fault locator settings and any post-processing of the fault locator output.

Section V shows how to use line taps to improve tower mapping accuracy on the per-unit scale. Towers with taps become landmarks for interpreting fault-location results.

Section VI shows how to use fault locations that a line crew confirmed with high confidence as extra landmarks. This approach allows ongoing calibration of the fault-locating system with each new line fault that has been found with high confidence.

Section VII provides basic information on the Optical Time Domain Reflectometry (OTDR) tests used to commission and troubleshoot line fiber-optic cables, including Optical Ground Wire (OPGW), Optical Power Wire (OPPW), and All-Dielectric Self-Supporting (ADSS) cables. For brevity, we use the term OPGW in this paper, even though most of our discussion applies to all three types of fiber cables. An OTDR test measures the distance to some splices along the line path. OTDR reports are available from OPGW commissioning or any major troubleshooting effort for an in-service fiber cable.

Section VIII shows how to use the OTDR results to develop additional power line landmarks and improve accuracy for dispatching line crews.

The paper includes five examples to better explain and illustrate the presented concepts.

II. TW Fault Locating for Power Lines

A. Principle of Operation

Fig. 1 shows a Bewley diagram for a fault at location F on a line of length LL. The fault is M (km or mi) away from the local terminal S and LL – M (km or mi) away from the remote terminal R. Faults launch TWs that propagate with a velocity (PV) in overhead lines of about 97 to 98 percent of the speed of light in free space. TW propagation velocity in cable lines is about 50 to 70 percent of the speed of light.

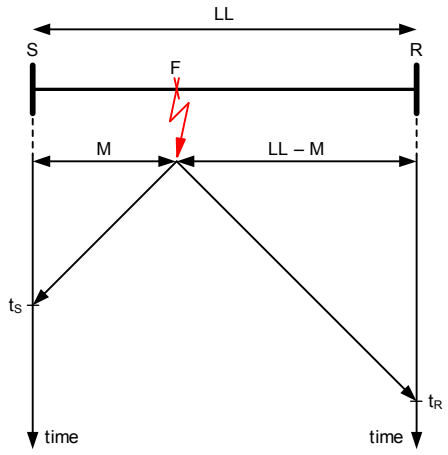

Fig. 1. Bewley diagram explaining the double-ended TW fault-locating method.

The fault at location F launches a TW toward the local terminal S. Counting from the fault inception time, this TW arrives at terminal S at t_S, traversing the total distance M:

$$M = t_S \cdot PV \tag{1a}$$

Similarly, the fault launches a TW that arrives at the remote terminal R at t_R, traversing the total distance LL – M:

$$LL - M = t_R \cdot PV \tag{1b}$$

We solve (1) for M assuming LL and PV to be known constants (settings) and t_S and t_R to be measurements taken for the fault, and we obtain:

$$M = \frac{1}{2}(LL + (t_S - t_R) \cdot PV) \tag{2}$$

Equation (2) is the operating principle of the double-ended TW fault-locating method. Double-ended TW fault locators [2] [3] capture time stamps of the first TWs at both line terminals in reference to a common time base, such as GPS-based absolute time; exchange the time stamps via a communications channel; and use (2) to calculate fault location.

Equation (2) contains the TW propagation velocity (PV) and the total line length (LL). These two values are not easy to measure. In contrast, we can measure the TW line propagation time (TWLPT), the time it takes for a TW to travel from one line terminal to the other line terminal. When commissioning a TW fault locator, we perform a line energization test to measure TWLPT with high accuracy [4] (see Section III). Having the TWLPT value, we substitute:

$$PV = \frac{LL}{TWLPT} \tag{3}$$

into (2), and we obtain:

$$M = \frac{LL}{2}\left(1 + \frac{t_S - t_R}{TWLPT}\right) \tag{4}$$

Further, we observe that the fault location M in physical units (km or mi) is the product of the total line length LL and the per-unit fault location m:

$$M = m \cdot LL \tag{5a}$$

$$m = \frac{1}{2}\left(1 + \frac{t_S - t_R}{TWLPT}\right) \tag{5b}$$

Equation (5) allows us to decouple the per-unit fault location, which depends only on time and the location in physical units. We can make the following observations relevant to our discussion on accuracy:

- The per-unit fault location m (5b) depends on the ratio of two times: the difference in the TW arrival times (the measurement) and the TW line propagation time (the setting).
- Both of the times that are involved in calculating the per-unit fault location (the measurement and the setting) are typically very accurate, with errors on the order of 1 μs or less. This high accuracy of the inputs to (5b) results in very high accuracy of the per-unit fault location m (see Subsection B for more details).
- When we convert the per-unit fault location m to the fault location in physical units M, we use the total line length LL as a multiplier in (5a). Because LL is

typically not known with high accuracy (see Section III), this calculation decreases the accuracy of M compared with the inherently higher accuracy of m.

- The double-ended TW fault locator works naturally in per-unit values obtained exclusively from time values. As we will see in this paper, using the per-unit output from a TW fault locator will allow us to retain the inherent accuracy and improve the accuracy of the crew dispatch.

Double-ended TW fault locators follow a very robust operating principle that requires them to capture and time-stamp only the first TWs at each line terminal [1]. Even though they require time synchronization and communications, they are the most widespread TW fault locator type today. Recently, single-ended TW fault locators integrated with line protective relays became available [2]. We will briefly review the operating principle of the single-ended method to show that the same key observations apply to both methods.

Fig. 2 shows a Bewley diagram for a fault on the line. The single-ended method captures and time-stamps the first TW launched by the fault (t_1 time stamp) as well as the first reflection from the fault (t_2 time stamp). Identifying the first reflection from the fault is challenging, but it is not a subject of this paper (see [4] for more information).

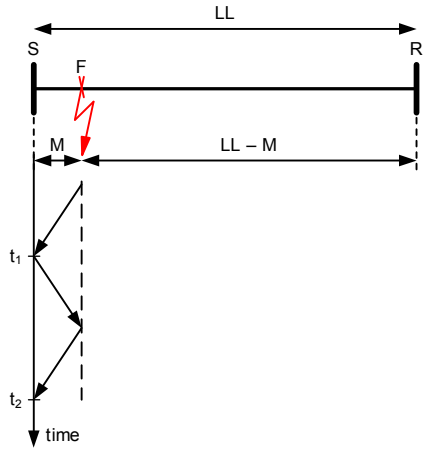

Fig. 2. Bewley diagram explaining the single-ended TW fault-locating method.

Between t_1 and t_2, the TW in Fig. 2 traveled from the local terminal to the fault and back to the local terminal. Therefore, we can write:

$$2 \cdot M = (t_2 - t_1) \cdot PV \tag{6}$$

Eliminating PV using (3) and solving for M, we obtain:

$$M = \frac{LL}{2}\left(\frac{t_2 - t_1}{TWLPT}\right) \tag{7}$$

We can separate the line length LL, the fault location in physical units M, and the per-unit fault location m as follows:

$$M = m \cdot LL \tag{8a}$$

$$m = \frac{1}{2}\left(\frac{t_S - t_R}{TWLPT}\right) \tag{8b}$$

As in the case of the double-ended method, the per-unit fault location m (8b) depends on the ratio of the measured time difference (in the case of the single-ended method, both time stamps are measured at the same terminal) and the TW line propagation time, TWLPT.

B. Accuracy Considerations

The double-ended and single-ended TW fault-locating methods share the same characteristics when it comes to error analysis and accuracy.

We use equations (4) and (7) to analyze the fault-locating errors and obtain the following rules regarding sensitivity to errors in the fault locator measurements (time-stamping) and settings:

- An LL setting error of 1 percent results in a fault-locating error of 1 percent.
- When using the double-ended method, a TWLPT setting error of 1 µs results in a fault-locating error of as much as 150 m (500 ft) for overhead lines and as much as 75 m (250 ft) for underground cables.
- When using the single-ended method, a TWLPT setting error of 1 µs results in a fault-locating error of as much as 300 m (1,000 ft) for overhead lines and as much as 150 m (500 ft) for underground cables. The difference between the double- and single-ended methods is a result of equations (4) and (7) using the TWLPT value in slightly different ways.
- A time-stamping error of 0.1 µs results in a fault-locating error of about 15 m (50 ft) on overhead lines and about 7.5 m (25 ft) on underground cables. When tested under ideal conditions for an overhead line, one fault locator [2] yields a 90th percentile error of less than 20 m (66 ft) and a median error of less than 10 m (33 ft).
- The overhead line conductor sag is approximately 0.3 percent of the line length. The sag changes with ambient temperature and line loading, resulting in line length changes of a fraction of the 0.3 percent value. As a result, you may expect an extra fault-locating error of a fraction of 0.3 percent.

You can obtain the TWLPT setting with 1 µs accuracy and the fault locator can time-stamp the TWs with submicrosecond accuracy. Therefore, the line length is the single largest component in the TW fault-locating error. This includes both the length at any given reference condition as well the length variability (sag changes due to variable loading and ambient conditions). For example, assume a 1 percent error in the line length setting and a fault located at a distance of 75 mi. The fault-locating error resulting from inaccuracy of the line length is 0.01·75 mi = 0.75 mi or 4,000 ft. This is four times a typical tower span, or four times a typical combined TWLPT and time-stamping error.

Impedance-based fault locators exhibit much higher inherent errors than TW fault locators. These inherent errors make the line length error negligible by comparison. Therefore, historically, our industry has not addressed the line length accuracy problem. However, the quest for improved line length accuracy would be misplaced. As we will show in this paper, what we need is not the end-to-end line length but a method to allocate tower positions to their per-unit locations. But first let us examine the line length concept in more detail.

III. Distance and Tower Positions

A. Line Length

We can define and measure the *length* of a power line in various ways.

1) Impedance

Distance protection elements and impedance-based fault locators are concerned with the line electrical length as defined by the apparent impedance. During line commissioning, we measure the line impedance by shorting one line end and applying a source at the system nominal frequency at the other end. In reference to Fig. 3, when we apply a positive-sequence voltage, we measure the positive-sequence impedance of the line ($Z_1 = V_1/I_1$), and when we apply a zero-sequence voltage, we measure the zero-sequence impedance of the line ($Z_0 = V_0/I_0$). These two complex numbers (Z_1 and Z_0) define the electrical line length as a relationship between voltages and currents at the line terminals. When defined this way, the electrical length is unambiguous and relatively accurate (the effects of line transposition and mutual coupling notwithstanding). Of course, this electrical length applies to methods that use fundamental frequency phasors, such as distance elements and impedance-based fault locators.

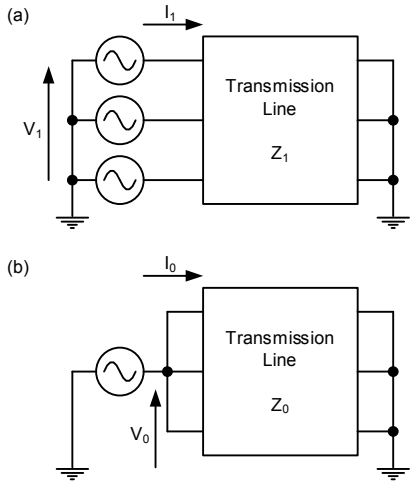

Fig. 3. Measuring line impedances during line commissioning: positive-sequence (a) and zero-sequence (b).

2) Traveling-Wave Line Propagation Time

TW protection elements and TW fault locators are concerned with the line electrical length as defined by the propagation velocity and time. During commissioning of a TW relay or a TW fault locator, we can perform a line energization test to measure the TW line propagation time. In reference to Fig. 4, we energize the line by closing a circuit breaker (CB). Closing a CB pole applies a step voltage to the line and launches a current TW. This current TW arrives at the remote terminal and completely reflects from the open end of the line. It then returns back to the first terminal with its polarity inverted. We know the line length with some accuracy and can approximate the propagation velocity reasonably well. Therefore, we calculate the expected round-trip time $t_{RT(EST)}$ for the TW during the line energization test as follows:

$$t_{RT(EST)} = \frac{2 \cdot LL}{PV} \tag{9}$$

We inspect the high-resolution event record of line energization to find a TW that arrived with inverted polarity around $t_{RT(EST)}$ after the first TW launched by the CB closure. Each pole closure would generate a new TW, providing a chance to measure the propagation time up to three times for each CB pole closure. We then measure the actual time difference between the two TWs, $t_{RT(MEAS)}$. Some viewing and analysis software programs for TW records [2] provide tools for accurate measurement of the difference in the TW arrival times, with resolution significantly better than 1 μs. The one-way TW line propagation time that the fault locator needs as a setting is half the round-trip time that we measured:

$$TWLPT = 0.5 \cdot t_{RT(MEAS)} \tag{10}$$

See [2] for more details and best practices on performing the TW line propagation time measurement.

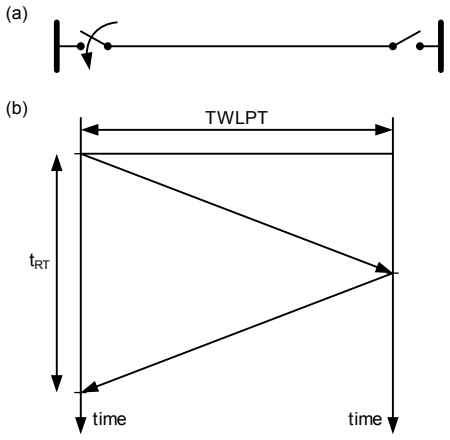

Fig. 4. Measuring TW line propagation time: the test (a) and Bewley diagram (b).

TW line propagation time is a form of electrical line length (similar to line impedances). TW line propagation time is unambiguous and directly measurable. As such, it is preferred over the TW propagation velocity PV, which is not directly measurable but must be calculated using (3). Moreover, when calculated, the propagation velocity depends on the physical line length LL. Any refinements to the LL value trigger corresponding changes to the PV value.

3) Physical Length

The physical line length LL is understood as a physical distance (km or mi) from one line end to the other. Fig. 5 illustrates the overhead line length ambiguity by depicting four

different definitions of distance between two adjacent towers [5]:

- d_1 is the length of the power conductors, which depends on their sag and may change with ambient temperature and line loading. This distance is probably the most accurate measure of the distance TWs travel.
- d_2 is the straight-line distance between the insulators. This distance is fixed and reflects the terrain elevation, but it neglects the conductor sag. Because OPGW conductors exhibit only a little sag, d_2 is representative of the length of the OPGW. The d_2 distance can be measured during or after line construction using laser distance measuring equipment at the bottom of the towers (assuming the terrain allows a line of sight).
- d_3 is the distance between the towers neglecting terrain elevation. This distance may be the easiest to measure from two-dimensional mapping data such as high-resolution aerial photos.
- d_4 is the actual distance between towers measured on the terrain surface. This distance may be the most accurate measure of the distance for a foot patrol but is not a practical distance measure for dispatching a line crew in today's world.

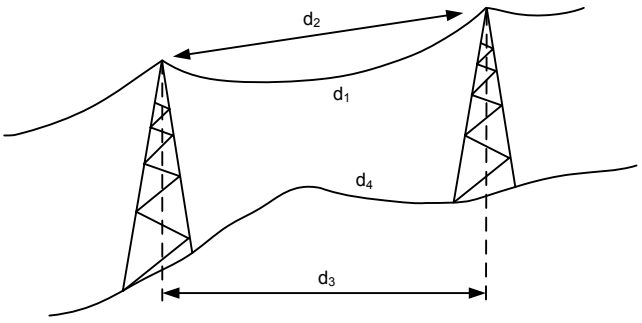

Fig. 5. Four different definitions of length for an overhead power line [5].

You can obtain the d_3 and d_4 values from your tower mapping data (position and elevation), but these values may not be accurate enough to preserve the inherent per-unit accuracy of the TW fault locators. The d_1 and d_2 distances are more accurate but are not easy to obtain.

In theory, we could apply time-domain reflectometry (TDR) to measure the electrical distance using a known propagation velocity of the TDR test pulses. But unlike the line impedance measurement or TW line propagation time measurement, such a test is not performed as a part of line commissioning, and it would be expensive. As we will see later in this paper, we can use line faults as "natural TDR tests" to obtain the total d_1 distance from the line terminal to the tower with the fault. We will also use OTDR tests for the OPGW fibers to obtain a distance similar to the d_2 distance.

B. Line Survey

Today, it is possible to survey high-voltage power lines with high accuracy. A high-accuracy line survey may be available for new lines as part of the line construction effort. You can perform a line survey for old lines or contract it out.

Referring to Fig. 5, you can obtain the d_2 or d_3 tower-to-tower distances using GPS-based surveying systems, such as the one explained in [6]. These systems use differential GPS augmentation to obtain a horizontal accuracy on the order of ±(0.25 m plus 1 ppm) and a vertical accuracy on the order of ±(0.5 m plus 1 ppm). When measuring a tower-to-tower distance of about 300 m, the 1 ppm error is only 0.0003 m and can be neglected. These accuracies are adequate to build a tower position table, needed for accurate TW fault locators. The position of the n-th tower is the sum of tower-to-tower distances from the first tower to the n-th tower. It is justified to assume that the mentioned positioning errors of ±0.25 m horizontal and ±0.5 m vertical are either random errors or systemic offsets. As a result, the error in the sum of tower-to-tower distances will tend to cancel.

You can also obtain d_2 distances using an optical surveying system, such as the one explained in [7]. These systems claim a distance accuracy of a few millimeters plus 2 ppm and have a range well exceeding a typical tower span. You will need a line of sight to use these systems, which sometimes can be a problem.

Many optical surveying systems allow angle measurements to a conductor. As a result, they allow measuring line sag and thus obtaining the d_1 distance in Fig. 5.

Using today's technology, a line survey produces high-accuracy tower position data, but it can be time consuming and relatively expensive. The methods described in this paper are cost-effective alternatives to a line survey and provide a means to double-check the survey data.

C. Tower Positions

When dispatching a crew to find a fault, it is important to realize that we are interested not in the total distance from a given substation to the fault but in the position of the tower nearest to the fault. Utilities use various mapping systems, most recently GPS coordinates, to identify tower positions. GPS coordinates are especially convenient because GPS locators and navigation systems are now commonly integrated with mobile phones and vehicles.

We do not perform foot patrols anymore and do not need the *distance to the fault*. Rather, we need the *fault position*. Practically, it means we need a tower identifier (ID) based on the fault-locating calculations so that we can query our tower position database to find GPS coordinates of the tower where the fault is.

Fig. 6 presents the crew dispatch process we recommend.

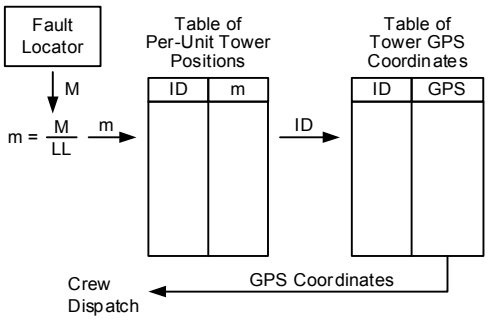

Fig. 6. Recommended crew dispatch process.

A typical fault locator provides the distance to the fault M in physical units assuming an end-to-end line length LL. We convert M to a per-unit fault location m (m = M/LL). This way we eliminate the dependence on the unreliable LL data. Next, we search the table of tower locations for m and obtain the ID of the tower nearest to the fault. We then use the tower ID to search the table of tower GPS positions to obtain the fault location in terms of GPS coordinates (or any other mapping system of choice). This is a simple process, but it requires a table that has the per-unit positions of the towers. In order to preserve the inherent accuracy of the TW fault locators, we need tower positions on the per-unit scale with accuracy better than approximately one-fourth or one-fifth of the TW fault locator accuracy, i.e., on the order of 50 m or 200 ft. If we work with per-unit locations and assume a 100 mi line, we need per-unit tower positions with accuracy on the order of 0.003 pu. In other words, we need to operate with four decimal places of resolution on the per-unit scale.

Note that the process in Fig. 6 works with either the per-unit distance m or the physical distance M. However, the distance M in physical units assumes the total line length LL. Because that value is not necessarily accurate and may be revised for other reasons over time, we recommend not using M, but using the per-unit distance m. This way, the line is characterized only by the TWLPT parameter – a value that is unambiguous and directly measurable.

IV. Line-End Considerations

Before we explain methods for obtaining the table of tower positions on the per-unit distance scale, let us discuss the distance, length, and TW line propagation time at the line ends.

A. Distances Within the Substation

To maximize the inherent accuracy of TW fault locators, we need to account for the following distances within the substation or just outside of the substation perimeter (see Fig. 7):

- The distance between the first tower of the line and the current transformer (CT) used by the fault locator, $d_{LINE-CT}$. This distance is not necessarily negligible compared with the inherent TW fault locator accuracy, and therefore you may need to consider it. The line CT connection is typically air-insulated, and the corresponding TW travel time ($t_{LINE-CT}$) can be estimated using the same propagation velocity as for the line. If the connection is gas-insulated (SF_6) or a cable (to solve the switchyard congestion), you must use the propagation velocity adequate for the medium (SF_6, cable) to obtain the $t_{LINE-CT}$ time.
- The distance between the CT and the fault locator, d_{CT-FL}. This distance is also not necessarily negligible compared with the inherent TW fault locator accuracy, and therefore you may need to consider it. If this distance is the same at both line ends, then you can neglect it. The CT cables have a TW propagation velocity of about 60 to 70 percent of the speed of light in free space. Therefore, these cables would appear to the TW fault locator applied to an overhead line as 40 to 70 percent longer than they actually are. We denote the travel time in CT cables as t_{CT-FL}.

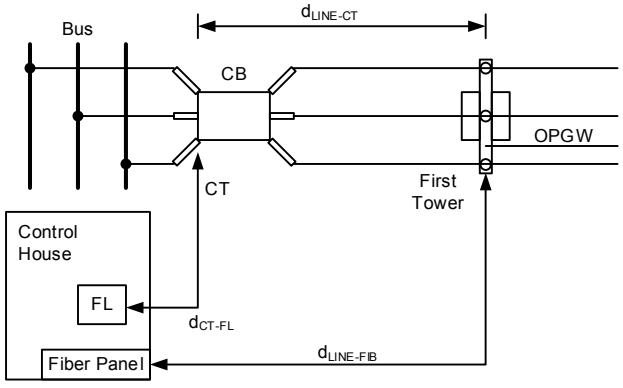

Fig. 7. Line-end considerations: distances between the first tower, CB, CT, fault locator, and fiber patch panel.

Let us also introduce the distance of a fiber cable (the *approach cable*) between the splice to the OPGW fiber at the first tower and the patch panel in the control building, $d_{LINE-FIB}$. We will account for this distance when using the OTDR commissioning report to find tower positions (see Section VIII).

Let us consider the line energization test in the context of line ends (see Fig. 8). The remote end will typically be open at the line disconnect switch or the CB. The distance between the disconnect switch (or CB) and the CT is typically small, and we can assume that the TW line propagation time we measure includes the $t_{LINE-CT}$ time at the remote line end. Account for any differences if the disconnect switch at the remote line end is located a relatively long distance away from the CT.

When we close the local CB, we launch the TW along the line toward the remote end. At the same time, we launch a secondary TW in the CT cables that travels the d_{CT-FL} distance between the CT and the fault locator. When the reflection from the remote end arrives, it is also delayed by the time to travel the same (d_{CT-FL}) distance before it reaches the fault locator. As a result, the line energization test measures the TW line propagation time between the local CB (CT, strictly speaking) and the remote CB (disconnect switch, strictly speaking). This TWLPT measurement *includes* the $d_{LINE-CT}$ distances at both ends and it *excludes* the d_{CT-FL} CT cable distances at both ends.

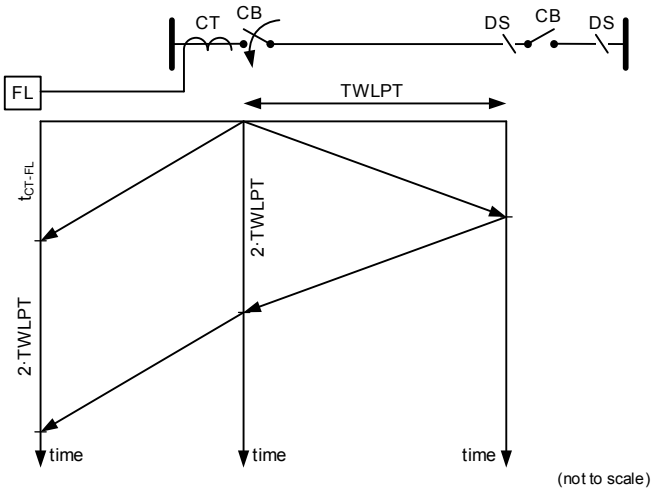

Fig. 8. Line energization test considering line end details.

Some TW fault locators [2] provide settings for compensating for the CT cable leads, i.e., for the t_{CT-FL} times at both line ends. They compensate by backdating the measured time stamps as follows:

$$m = \frac{1}{2}\left(1 + \frac{(t_S - t_{CT-FLS}) - (t_R - t_{CT-FLR})}{TWLPT}\right) \quad (11a)$$

We can rearrange (11a):

$$m = \frac{1}{2}\left(1 + \frac{(t_S - t_R) - (t_{CT-FLS} - t_{CT-FLR})}{TWLPT}\right) \quad (11b)$$

From (11), we realize that the effective compensation is for the difference in the CT cable lengths and not for the individual lengths at both line terminals. Therefore, the compensation is not needed if the CT cable lengths are the same or similar at both line ends.

B. Position of the First Tower

If you measure the TWLPT parameter (setting) using the line energization test, you obtain the TW line propagation time between the two CTs of the line and not between the first two towers at the line ends. Let us calculate the positions of the first towers at the line ends.

If you use CT cable compensation (11)

The local CT is at the per-unit distance m = 0 pu. Therefore, the 1 pu length spans from the local CT to the remote CT.

The per-unit distance m_1 of the first tower is the following:

$$m_1 = \frac{t_{LINE-CT}}{TWLPT} \quad (12)$$

If you do not use CT cable compensation (5b)

The per-unit distance $m_{CT(LOC)}$ of the local CT is the following:

$$m_{CT(LOC)} = \frac{t_{CT-FL(LOC)} - t_{CT-FL(REM)}}{2 \cdot TWLPT} \quad (13)$$

Note that if the remote CT cable is longer than the local CT cable, the local CT will appear at a negative per-unit location.

The per-unit distance m_1 of the first tower is the following:

$$m_1 = \frac{t_{LINE-CT}}{TWLPT} - \frac{t_{CT-FL(LOC)} - t_{CT-FL(REM)}}{2 \cdot TWLPT} \quad (14)$$

Use Bewley diagrams to derive and understand equations (13) and (14).

Calculate the per-unit position of the first tower at each line end using (12) or (14) and use the first towers as landmarks. By a landmark, we mean a point with a position on the per-unit scale that is known with high confidence and accuracy and will not be further adjusted based on finding other landmarks.

Consider the following example.

Example 1

Table I shows the TWLPT value we obtained from the line energization test. Assuming the propagation velocity of 97 percent of the speed of light in free space, this line is approximately 45.3 km long. We used the distances from the CT to the first tower noted on the substation switchyard drawings. We also used the drawings to approximate the length of the CT cables. We calculated the propagation times between the CTs and the first towers using 97 percent of the speed of light and in the CT cables using 70 percent of the speed of light.

TABLE I
EXAMPLE 1 INPUT DATA

Variable	Local	Remote	Source of Data
TWLPT	155.846 μs		Measured
$d_{LINE-CT}$	175 m	255 m	Switchyard drawing
d_{CT-FL}	253 m	125 m	Switchyard drawing
$t_{LINE-CT}$	0.602 μs	0.877 μs	Calculated, 0.97·c
t_{CT-FL}	1.206 μs	0.596 μs	Calculated, 0.70·c

Assume first that we used the 1.206 μs and 0.596 μs values as settings to compensate for the CT cable length. According to (12), the first towers are located at 0.0039 pu and 0.0056 pu at the local and remote terminals, respectively.

Assume next that we did not use the CT cable compensation settings. According to (13), the CTs are located at 0.0020 pu and –0.0020 pu at the local and remote terminals, respectively. According to (14), the first towers are located at 0.0019 pu and 0.0076 pu at the local and remote terminals, respectively.

This example shows that there will be a slight difference in tower locations impacting the overall accuracy of fault locating depending on whether or not you compensate for the CT cables. In our example, the difference is about 0.0020 pu or 0.0020·45.3 = 0.09 km or 90 m (a third of a tower span).

Using the methods described in this paper, you can correctly locate towers on the per-unit scale, choosing whether or not to apply the CT cable compensation. However, the per-unit scale is more logical if you use CT cable compensation (the local CT/CB is at 0 pu and the remote CT/CB is at 1 pu). Also, to avoid confusion, it is beneficial to use the same approach (with or without CT cable compensation) across all your applications. Therefore, we recommend using CT cable compensation in all

applications (unless the CT cable lengths are equal at both line ends, and then the compensation is not needed). We will describe the methods for finding tower positions assuming the CT cable compensation is applied.

C. Converting Default Tower Positions to Per-Unit Positions

Assume your line has N towers, where n = 1 is the first tower and n = N is the last tower (the first tower as seen from the other line end). Prepare a table of distances in km or mi from the local line end to all towers (M table). Of course, $M_{(1)} = 0$ km or mi and $M_{(N)}$ = LL km or mi. You can obtain the M table from the line files.

Our objective is to calculate the per-unit tower location table (m table). Using (12), we already found the per-unit positions of the first towers at each substation: $m_{(1)} = m_{1LOC}$ and $m_{(N)} = 1 - m_{1REM}$. The value of $m_{(1)}$ is not exactly 0 pu because 0 pu is the location of the local CB/CT. The value of $m_{(N)}$ is not exactly 1 pu because 1 pu is the location of the remote CB/CT. Apply a straight proportionality to convert the M table into the m table:

$$m_{(k)} = m_{(1)} + \frac{M_{(k)}}{M_{(N)}}\left(m_{(N)} - m_{(1)}\right) \tag{15}$$

Consider the following example.

Example 2

The line of Example 1 has N = 151 towers (Table II) and a line length LL of 45.321 km counted from the first tower to the last tower. From Example 1, the first towers are located at 0.0039 pu from the local end and 0.0056 pu from the remote end (or 1 – 0.0056 pu = 0.9944 pu from the local end). These towers are landmarks and we show them in bold font in Table II. Using (15), we convert the tower locations in physical units M into per-unit locations m. Table II shows the results of the calculations.

Referring to the process of Fig. 6, if a line fault occurs and the fault locator outputs m = 0.4425 pu, we will inspect Tower 68 (0.4421 pu) and one or two adjacent towers on both sides of Tower 68.

TABLE II
EXAMPLE 2: TOWER LOCATION DATA

Tower ID	Span (m)	M (km)	m (pu)
1	0	0.000	**0.0039**
2	256	0.256	0.0095
3	304	0.560	0.0161
4	310	0.870	0.0229
5	287	1.157	0.0292
…			
31	286	8.967	0.1999
32	309	9.276	0.2066
33	310	9.586	0.2134
34	275	9.861	0.2194
35	299	10.16	0.2259
…			
65	302	19.133	0.4221
66	303	19.436	0.4287
67	315	19.751	0.4356
68	301	20.052	0.4421
69	280	20.332	0.4483
70	300	20.632	0.4548
…			
146	308	43.781	0.9607
147	308	44.089	0.9675
148	306	44.395	0.9742
149	310	44.705	0.9809
150	313	45.018	0.9878
151	303	45.321	**0.9944**

V. LINE TAPS AS LANDMARKS

A line tap is a natural landmark. A tap creates a discontinuity in the line characteristic impedance and reflects TWs. By identifying reflections from the tap and time-stamping them, you can measure the per-unit distance to the tap during line energization or during a suitable natural event such as an internal or external fault. Fig. 9 shows the Bewley diagram for an energization test of a line with a tap.

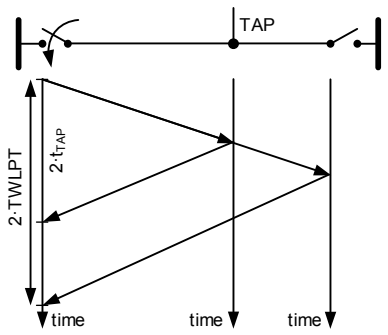

Fig. 9. Bewley diagram for line energization of a tapped line.

You can measure the round trip to the tap, $2 \cdot t_{TAP}$, and calculate the per-unit position of the tower with the tap as:

$$m_{TAP} = \frac{t_{TAP}}{TWLPT} \tag{16}$$

Consider the following example.

Example 3

Assume the line in Table II has a tap at Tower 67. A line energization test allowed us to measure TWLPT = 155.846 μs and t_{TAP} = 68.874 μs. Using (16), we calculate the accurate per-unit position of Tower 67 to be 0.4419 pu (the previously best-known position of Tower 67 was 0.4356 pu according to Table II). Using the 0.4419 pu value as a new landmark, we recalculate the positions of all the towers as follows:

$$m_{NEW(67)} = 0.4419 \text{ pu} \tag{17a}$$

Towers 2 to 66:

$$m_{NEW(k)} = m_{(1)} + \frac{m_{NEW(67)} - m_{(1)}}{m_{(67)} - m_{(1)}}\left(m_{(k)} - m_{(1)}\right) \tag{17b}$$

Towers 68 to 150:

$$m_{NEW(k)} = m_{(151)} + \frac{m_{NEW(67)} - m_{(151)}}{m_{(67)} - m_{(151)}} \cdot \ldots \\ \ldots \cdot \left(m_{(k)} - m_{(151)}\right) \tag{17c}$$

Equation (17) repositions all towers between the new landmark (Tower 67) and the adjacent landmarks (Tower 1 and Tower 151). After applying (17), the line has three landmarks: Tower 1 (0.0039 pu), Tower 67 (0.4419 pu), and Tower 151 (0.9944 pu); all the other towers are repositioned between the landmarks in proportion to the previously known spacing between the towers. Table III shows the previously best-known tower positions and the positions updated to account for the new landmark at Tower 67 (the tap location).

TABLE III
EXAMPLE 3: UPDATED TOWER LOCATION DATA USING A LINE TAP AS A LANDMARK

Tower ID	m (pu)	m_{NEW} (pu)
1	**0.0039**	**0.0039**
2	0.0095	0.0096
3	0.0161	0.0163
4	0.0229	0.0232
5	0.0292	0.0296
…		
31	0.1999	0.2028
32	0.2066	0.2096
33	0.2134	0.2165
34	0.2194	0.2225
35	0.2259	0.2291
…		
65	0.4221	0.4282
66	0.4287	0.4349
67	0.4356	**0.4419**
68	0.4421	0.4483
69	0.4483	0.4545
70	0.4548	0.4609
…		
146	0.9607	0.9611
147	0.9675	0.9678
148	0.9742	0.9744
149	0.9809	0.9811
150	0.9878	0.9879
151	**0.9944**	**0.9944**

In Table III, the tower positions near the new landmark have changed the most (Tower 67 was repositioned by 0.0063 pu or about one tower span). The tower positions near the previous landmarks have changed the least. The positions of the previous landmarks (Tower 1 and Tower 151) have not changed at all.

VI. CONFIRMED FAULT LOCATIONS AS LANDMARKS

You can use a confirmed fault location as a natural line TDR test to find the per-unit location of the tower with the fault. In many cases, line crews find the fault with very high confidence, such as by discovering a foreign object still touching power conductors or lying beneath the line, a clearly damaged insulator, and so on. Assume the crew found a fault at Tower n corresponding to the tower location $m_{(n)}$ in the table of per-unit tower positions and the fault locator reported m_{FLT}. If the two locations do not differ too much, such as they are within 1 to 2 tower spans from each other, you may consider that Tower n is truly located at the per-unit distance m_{FLT} and you may reposition Tower n to location m_{FLT} in the table of per-unit tower positions. It is a good practice to inspect the fault record for fault precursors and any other high-frequency noise that could cause a TW fault-locating error. If you consider the TW fault-locating result m_{FLT} trustworthy, you may proceed with using it to create a new landmark.

Consider the following example.

Example 4

Assume the fault locator reported m_{FLT} = 0.2221 pu for the line in Table III and the crew found the fault with high confidence at Tower 32. As a result, you may introduce a new landmark at Tower 32 with the per-unit tower position of 0.2221 pu instead of the previously best-known Tower 32 position of 0.2165 pu.

Apply the following corrections:

$$m_{NEW(32)} = 0.2221 \text{ pu} \tag{18a}$$

Towers 2 to 31:

$$m_{NEW(k)} = m_{(1)} + \frac{m_{NEW(32)} - m_{(1)}}{m_{(32)} - m_{(1)}}\left(m_{(k)} - m_{(1)}\right) \tag{18b}$$

Towers 33 to 66:

$$m_{NEW(k)} = m_{(67)} + \frac{m_{NEW(32)} - m_{(67)}}{m_{(32)} - m_{(67)}}\left(m_{(k)} - m_{(67)}\right) \tag{18c}$$

Equation (18) repositions all towers between the new landmark (Tower 32) and the adjacent landmarks (Tower 1 and Tower 67). After applying (18), the line has a total of four landmarks: Tower 1 (0.0039 pu), Tower 32 (0.2221 pu), Tower 67 (0.4419 pu), and Tower 151 (0.9944 pu). Table IV shows the previously best-known tower positions and the positions updated to account for the new landmark (the per-unit location of Tower 32 determined by the fault found at this tower).

TABLE IV
EXAMPLE 4: UPDATED TOWER LOCATION
DATA USING A FAULT LOCATION AS A LANDMARK

Tower ID	m (pu)	m_{NEW} (pu)
1	**0.0039**	**0.0039**
2	0.0096	0.0099
3	0.0163	0.0171
4	0.0232	0.0244
5	0.0296	0.0312
…		
31	0.2028	0.2149
32	0.2096	**0.2221**
33	0.2165	0.2286
34	0.2225	0.2343
35	0.2291	0.2406
…		
65	0.4282	0.4289
66	0.4349	0.4353
67	**0.4419**	**0.4419**
68	0.4483	0.4483
69	0.4545	0.4545
70	0.4609	0.4609
…		
146	0.9611	0.9611
147	0.9678	0.9678
148	0.9744	0.9744
149	0.9811	0.9811
150	0.9879	0.9879
151	**0.9944**	**0.9944**

In Table IV, the tower positions near the new landmark have changed the most (Tower 32 was repositioned by 0.0056 pu or about one tower span). The tower positions near the previous landmarks (Tower 1 and Tower 67) have changed the least. The positions of the previous landmarks and the towers between Tower 67 and Tower 151 have not changed at all.

VII. OPGW FIBER COMMISSIONING AND TROUBLESHOOTING

OPGW fiber is a very valuable asset that is costly to install. After installation, the ground wire is checked and commissioned using a wide range of tests [8]. Fiber commissioning and troubleshooting tests almost always include OTDR tests.

An OTDR test launches a short light pulse of a known power and measures the power and timing of reflections from connectors, splices, bends, and defects. The primary objective of the test is to verify the fiber quality (no defects), the fiber losses, and the quality of the connections (both splices and plug-in connectors). The test also locates points that cause measurable reflections (splices, patch panels, optical amplifiers, unintended sharp bends, or pinch points). The OTDR test for an OPGW fiber can be better understood in reference to Fig. 10.

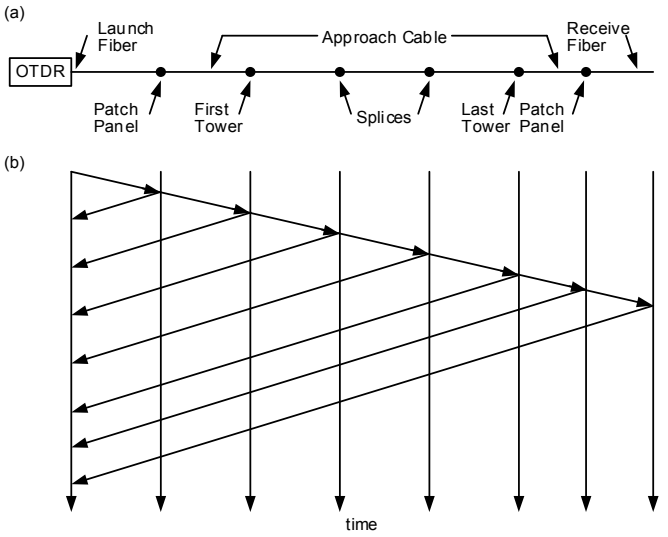

Fig. 10. OTDR test setup (a) and Bewley diagram (b).

The OTDR test unit launches a short light pulse of a certain wavelength. Typically, the test is run twice with pulses of 1,310 nm and 1,550 nm wavelengths. The pulse is relatively short, on the order of 10 μs. In order to measure the very first connection at the fiber patch panel, a *launch fiber* is used. The role of the launch fiber is to provide enough delay for the OTDR laser to finish producing the test pulse and for the OTDR photo detector to be ready to measure the reflection from the first connection at the patch panel. Given the speed of light in fiber and the 10 μs typical pulse duration, the launch fiber is typically about 1 km long. The launch fiber is a single fiber (not a pair) and does not need a jacket. As a result, a typical launch fiber fits in a small chassis and is an accessory to the OTDR meter. Likewise, in order to measure the last connection, a *receive fiber* is connected at the end of the tested fiber.

Typically, the test is run from the fiber patch panel in the control house and it covers the following sections and transition points:

- Local fiber patch panel.
- Local approach cable, including any extra length (slack) left for repairs.
- The splice between the approach cable and the OPGW at the first tower.
- Splices along the OPGW.
- The splice between the OPGW and the approach cable at the last tower in the remote substation.
- Approach cable at the remote substation, including any slack for repairs.
- Fiber patch panel at the remote substation.

Today's communications equipment lasers work for fibers up to about 100 km long. Longer OPGW sections would have

optical amplifiers or signal regenerators. For such lines, the OTDR tests are run to and between the amplifier locations.

Fig. 11 shows a typical plot from the OTDR test. The plot shows optical signal losses and reflection markers.

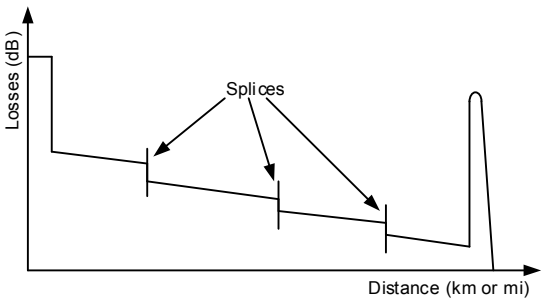

Fig. 11. Typical plot from an OTDR test.

Depending on the *splice loss threshold* test parameter (for example, 0.05 dB), the OTDR test can identify a number of splices. For each splice, it provides the signal loss measurement and location. In this paper, we are interested in the location of the splices. OTDR equipment may output splice location with a 0.1 m resolution and may have an effective distance accuracy on the order of 2.5 to 10 m.

An OPGW is a heavy composite cable that can be manufactured and transported in sections up to a certain length. The maximum OPGW length is on the order of 10 km. Typically, OPGW splices are 2 to 10 km apart, or 7 to 30 towers apart. These splices provide a great opportunity for using OTDR to find positions of many towers along the line.

A typical OTDR test report includes an *event table*. An event table summarizes the plot of Fig. 11 and is similar to Table II, but it includes locations of detected reflection points.

Expect to measure longer fiber lengths with the OTDR than conductor lengths. The following factors contribute to the difference:

- Fibers must not be mechanically stressed and therefore they have 1 to 2 percent of extra length compared with the aluminum tubing protecting them inside the ground wire. For a 100 km line, the extra 1 to 2 percent is 1 to 2 km or 3 to 6 tower spans.
- The splices are made close to ground for ease of access. As a result, the OPGW conductor is brought down and back up at each splice location (see Fig. 12). This extra length is approximately twice the tower height or about 2·(20 to 55) m. With 80 m of extra length per splice and 5 to 10 splices along the line, the extra length can be as much as 1 km for a long high-voltage line.
- An extra length (slack) is left at each splice for repairs (see Fig. 12).

However, we can justifiably assume that the per-unit location of splices is the same as the per-unit location of the towers with the splices. This is because the extra length of fibers in the aluminum tubing is distributed uniformly and the extra OPGW length at the splices is equal on both sides of the splice. This allows us to calculate per-unit positions of towers with splices as we explain in the next section.

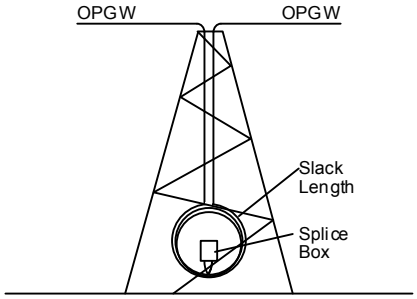

Fig. 12. Extra OPGW length at a splice tower.

VIII. OPGW Fiber Splices as Landmarks

A. Verifying OTDR Distance Measurements

Before you use tower locations obtained with an OTDR test, make sure these locations are accurate. Follow these best practices:

- Indicate the splice locations in the table of towers and use the table to eliminate any false positives such as fiber defects, bends with too short a radius, etc. Disregard any reflections (markers) that are too far from the known locations of splices based on the line construction record.
- Check the 1,310 nm and 1,550 nm test results for consistency. The 1,550 nm tests are typically more sensitive and may result in false positives. When they agree, average the 1,310 nm and 1,550 nm results for better accuracy.
- If you have test results for several fibers in the OPGW, check these results for consistency and average them for better accuracy.
- Collect as many OTDR reports as possible; check them for consistency, and average splice locations for better accuracy (OTDR tests are performed to troubleshoot issues, not only during commissioning after construction; often you have access to multiple test reports for the same fiber cable).
- To avoid a common-mode failure, a line protection system – possibly including a TW fault-locating function – may use the fiber connection on a line (path) parallel to the protected line. Remember to use the OTDR data for the fiber in the protected line's OPGW, not the fiber the fault locator is using.

B. Calculating Per-Unit OPGW Splice Locations

The OTDR event table may include the launch fiber length and may exclude the location of the first tower depending on the losses at the splice and the length of the approach cable. If the first splice does not have enough losses, it may not be visible. If the approach cable is short, the OTDR may fail to separate the reflection from the patch panel and the reflection from the first splice (see Fig. 10).

Knowing the length of the launch cable (d_{LAUNCH}) and the approach cable ($d_{LINE\text{-}FIB}$ in Fig. 7), you can shift locations of all identified splices to count the fiber length in reference to the first tower, as follows:

$$M_{SLPICE} = M_{SLPICE} - d_{LINE-FIB} - d_{LAUNCH} \quad (19)$$

Applying (19) for all identified splices provides their distances to the first tower.

In order to obtain the per-unit splice positions, you need the distance to the last tower, $M_{SPLICE(N)}$. This distance is the distance to the remote patch panel minus the length of the approach cable at the remote substation. In other words, it is the distance to the end of the receive fiber minus the length of the receive fiber and the length of the approach cable. You need to express the distance to the last tower in reference to the first tower, i.e., you need to apply (19) to $M_{SPLICE(N)}$.

Let us adapt (15) to convert the location of splices in km or mi into per-unit locations:

$$m_{SPLICE(k)} = m_{(1)} + \frac{M_{SPLICE(k)}}{M_{SPLICE(N)}}\left(m_{(N)} - m_{(1)}\right) \quad (20)$$

where $m_{(1)}$ and $m_{(N)}$ are the per-unit locations of the first and last towers, according to (12); k is the index of the identified splice locations; and $M_{SPLICE(N)}$ is the fiber distance to the last tower.

Consider the following example.

Example 5

Assume the line in Table II has an OPGW installed and the OTDR test identified splices at the locations shown in Table V. These locations are referenced to the first tower (resulting from applying (19)). Note that not all splices have been identified by the test. For example, the distance between Tower 47 and Tower 74 is about 17 km and it is too long to be a single OPGW section. There is at least one more splice between Tower 47 and Tower 74.

TABLE V
EXAMPLE 5: SPLICE LOCATIONS

Tower ID	M_{SPLICE} (km)	m (pu)	Comment
1	0.000	**0.0039**	First tower
47	5.180	0.1154	Splice
74	22.543	0.4893	Splice
101	30.768	0.6664	Splice
133	40.517	0.8763	Splice
151	46.002	**0.9944**	Last tower

Note that the OTDR-measured fiber length between Tower 1 and Tower 151 in our example is 46.002 km, compared with 45.321 km in Table II. This result is expected if the length in Table II relates to the physical distance between the towers (the fiber is 1 to 2 percent longer). Table V shows the landmarks of the first and last towers according to our earlier calculations with (12).

We use (20) to calculate the per-unit positions of the towers with splices. For example, Tower 133 is located at 0.8763 pu. Next, we consider Tower 1, Tower 47, Tower 74, Tower 101, Tower 133, and Tower 151 as landmarks and reposition all towers between each pair of landmarks proportionally, as we did in previous examples.

IX. CONCLUSIONS

The per-unit traveling-wave fault-locating calculation depends on the ratio of two times: a measurement and a setting. You can obtain the TW line propagation time setting with accuracy on the order of 1 μs or better by performing a line energization test. During faults, the TW fault locator measures the TW arrival times with submicrosecond accuracy. As a result, the fault location obtained with a TW fault locator is typically accurate to one tower span, but only if expressed in per unit.

To dispatch a line crew with maximum accuracy, we need a method to map the accurate per-unit fault location to a tower ID, and from there, to GPS coordinates. If we perform this mapping using crude estimates of tower positions, then we lose some of the inherent accuracy of TW fault locating.

Using today's technology, a line survey can provide precise tower locations, but it may be time-consuming and relatively expensive.

This paper presents several cost-effective approaches for improving the mapping of towers on the per-unit scale. We propose creating and refining a table of per-unit tower positions and using this table when converting the TW fault-location result to GPS tower coordinates for dispatching line crews.

We advise performing a line energization test to obtain the TW line propagation time setting for the fault locator. We explain how to account for the line-end effects including distances between the energizing CB, the CT used for measurement, and the fault locator itself. We advocate for applying CT cable length compensation so that the 0 to 1 pu line length scale spans from the local CB to the remote CB. You can use equations from this paper to develop an alternative convention where the 0 to 1 pu line length scale spans from the first tower to the last tower of the line.

We introduce the concept of landmarking for improving accuracy of fault locating. A landmark is a tower with a per-unit position that is known with high accuracy and confidence. We show how to reposition towers between any two landmarks based on their previously best-known positions for better fault-locating accuracy.

We show how to calculate the per-unit positions of the first tower (close to 0 pu) and the last tower (close to 1 pu) so that we can use them as landmarks, while accounting for distances between the first/last tower, the CT, and the TW fault locator.

We show how to create extra landmarks using taps on the line. We show how to use locations of past faults that line crews confirmed with high confidence as additional landmarks.

We also show how to use OTDR test results to convert towers with identified splices into new landmarks. This method is possible based on the fundamental observation that the per-unit optical TW distance (OTDR) and the per-unit electrical TW distance (fault) are the same. However, the physical distances of the OPGW fiber and the power conductors can differ. Therefore, apply care when operating in physical length units and using the OTDR distance measurements together with other types of distance measurements or data. To solve this difference in physical length, we advocate operating in per-unit values, taking the two CB positions as 0 pu and 1 pu.

Using the methods presented in this paper, you can obtain a landmark every several km or mi. Mapping the per-unit output from the TW fault locator using a nearby landmark to the tower ID and further to tower GPS coordinates allows us to retain the very high accuracy of TW fault locators and improve line crew efficiency for finding faults.

X. References

[1] E. O. Schweitzer, III, A. Guzmán, M. V. Mynam, V. Skendzic, B. Kasztenny, and S. Marx, "Locating Faults by the Traveling Waves They Launch," proceedings of the 40th Annual Western Protective Relay Conference, Spokane, WA, October 2013.

[2] *SEL-T400L Time-Domain Line Protection Instruction Manual*. Available: selinc.com.

[3] *SEL-T411L Advanced Line Differential Protection, Automation, and Control System Instruction Manual*. Available: selinc.com.

[4] E. O. Schweitzer, III, A. Guzmán, M. Mynam, V. Skendzic, B. Kasztenny, C. Gallacher, and S. Marx, "Accurate Single-End Fault Location and Line-Length Estimation Using Traveling Waves," proceedings of the 13th International Conference on Developments in Power System Protection, Edinburgh, UK, March 2016.

[5] B. Kasztenny, A. Guzmán, M. V. Mynam, and T. Joshi, "Locating Faults Before the Breaker Opens – Adaptive Autoreclosing Based on the Location of the Fault," proceedings of the 44th Annual Western Protective Relay Conference, Spokane, WA, October 2017.

[6] *SP80 GNSS Receiver Data Sheet*. Available: spectrageospatial.com.

[7] *FOCUS 35 Optical Surveying System Data Sheet*. Available: spectrageospatial.com.

[8] CIGRE Technical Brochure No. 746 "Design, deployment and maintenance of optical cables associated to overhead HV transmission lines," 2018, ISBN 978-2-85873-448-1.

XI. Biography

Bogdan Kasztenny has specialized and worked in power system protection and control since 1989. In his decade-long academic career, Dr. Kasztenny taught power system and signal processing courses at several universities and conducted applied research for several relay manufacturers. Since 1999, Bogdan has designed, applied, and supported protection, control, and fault-locating products with their global installed base counted in thousands of installations. Since 2009, Bogdan has been with Schweitzer Engineering Laboratories, Inc. where he works on product research and development. Bogdan is an IEEE Fellow, a Senior Fulbright Fellow, a Canadian representative of the CIGRE Study Committee B5, and a registered professional engineer in the province of Ontario. Bogdan has served on the Western Protective Relay Conference Program Committee since 2011 and on the Developments in Power System Protection Conference Program Committee since 2015. Bogdan has authored over 200 technical papers and holds over 40 patents.

20190404 • TP6915-01